New Journal of Physics
The open access journal for physics

Crystal and fluid modes in three-dimensional finite dust clouds

André Schella[1,5], Matthias Mulsow[1], André Melzer[1], Hanno Kählert[2,4], Dietmar Block[3], Patrick Ludwig[4] and Michael Bonitz[4]

[1] Institut für Physik, Ernst-Moritz-Arndt-Universität Greifswald, D-17489 Greifswald, Germany
[2] Department of Physics, Boston College—Chestnut Hill, MA 02467, USA
[3] Institut für Experimentelle und Angewandte Physik, Christian-Albrechts-Universität zu Kiel, D-24098 Kiel, Germany
[4] Institut für Theoretische Physik und Astrophysik, Christian-Albrechts-Universität zu Kiel, D-24098 Kiel, Germany
E-mail: schella@physik.uni-greifswald.de

New Journal of Physics **15** (2013) 113021 (17pp)
Received 30 August 2013
Published 11 November 2013
Online at http://www.njp.org/
doi:10.1088/1367-2630/15/11/113021

Abstract. The spectral properties of three-dimensional dust clusters confined in gaseous discharges are investigated using both a fluid mode description and the normal mode analysis (NMA). The modes are analysed for crystalline clusters as well as for laser-heated fluid-like clusters. It is shown that even for clusters with low particle numbers and under presence of damping fluid modes can be identified. Laser-heating leads to the excitation of several, mainly transverse, modes. The mode frequencies are found to be nearly independent of the coupling parameter and support the predictions of the underlying theory. The NMA and the fluid mode spectra demonstrate that the wakefield attraction is present for the experimentally observed Yukawa balls at low pressure. Both methods complement each other, since NMA is more suitable for crystalline clusters, whereas the fluid modes allow to explore even fluid-like dust clouds.

[5] Author to whom any correspondence should be addressed.

Contents

1. Introduction

One access to study the dynamics of finite systems are dusty plasmas (see [1–3] for an overview). These are plasmas with additionally embedded, typically micron-sized, particles. Once immersed in the discharge, the particles attain a high negative charge through the ion and electron fluxes to the particles' surface. Due to the high charge and a thermal energy near room temperature the dust system generally is strongly coupled. In dusty plasmas, the particle dynamics can be studied on the kinetic level of individual particles.

When the system consists of less than a thousand dust particles, it is often considered to be finite. Finite systems are known to differ from extended bulk matter in many ways. Theoretical concepts and quantities had to be developed to account for boundary-related effects dominating over volume effects [4–8].

In dusty plasmas, finite dust clusters can be formed by trapping the particles in a cubic glass box inside a discharge plasma [9–17]. There, the dust particles arrange under the influence of their mutual Yukawa interaction and a harmonic confinement into nested spherical shells, the so-called Yukawa balls [9, 10].

While the shell structure and energy states of finite three-dimensional (3D) dust clouds are well understood [18–26], the dynamical properties of finite 3D systems are less explored [14, 27–34]. They offer the possibility to study the interplay between the external confinement and the particle–particle interaction.

Two alternative approaches to study the mode dynamics of finite dust clouds have been put forward: the normal mode analysis (NMA) together with its offspring, the instantaneous NMA and, more recently, the fluid mode description. In the NMA approach, the particle dynamics is described as a harmonic oscillation pattern around the particles' equilibrium positions, the so-called eigenmodes of the system. The NMA has been applied to two-dimensional (2D) dust clusters [4, 35, 36]. So far, 3D systems have been investigated by NMA only at high gas pressure, where the modes are heavily damped [27].

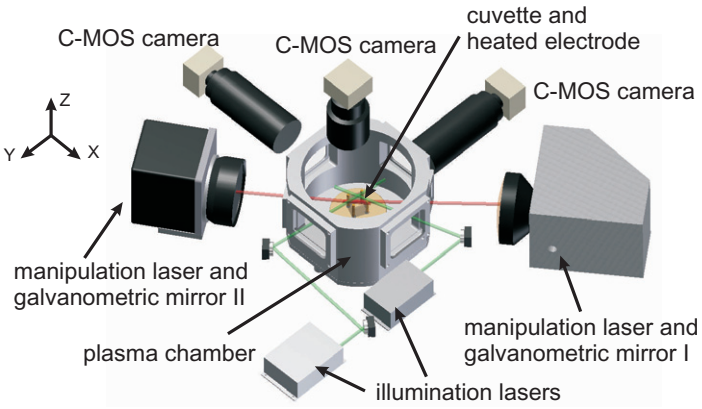

Figure 1. Scheme of the experimental setup. The particles confined in the glass box are illuminated by two Nd:YAG lasers from two sides and manipulated by two diode lasers from opposing directions. The three orthogonal high-speed cameras allow for a full 3D dynamic tracking of particle trajectories.

A different, recently developed approach has been proposed by Kählert and Bonitz [8, 37]. They have treated the Yukawa ball similar to a fluid droplet, deriving the fluid modes of a 3D dust cluster from a cold fluid plasma description.

In the following, we adopt both approaches to describe the dynamical properties of experimentally observed Yukawa balls. The scope is to compare fluid modes and NMA both for crystalline and liquid-like, laser heated clusters. The dust clouds under investigation are heated systematically and identically by means of two laser beams. Laser-heating enables to drive the clusters from a crystalline to a fluid-like state, and hence to study the mode dynamics over a wide range of the strong-coupling regime [14, 38–45].

The dust clouds are investigated at different gas pressures to study the influence of ion streaming motion on the mode properties. At low gas pressure the ion streaming motion leads to the onset of attractive forces between the dust particles [46–51].

Finally, NMA and fluid mode approach are compared to each other. Also, the limitations of the approaches are discussed in section 3.

2. Experiment

The experimental setup to trap 3D dust clusters has been described extensively in [13, 14, 23, 27] (see figure 1) and will only be briefly reviewed here. The experiments have been carried out in an asymmetric capacitively coupled rf discharge in argon. The rf power was varied between 1.2 and 1.5 W (corresponding to $U_{\mathrm{pp}} = 70$ and 95 V at the driven electrode), the neutral gas pressure was set to rather low values ranging between 4.8 to 7.8 Pa.

Inside a cubic glass box of 2.5 cm wall-length placed on a heated electrode, a small number of particles (melamine–formaldehyde particles of 4.86 μm in diameter) is trapped in a harmonic 3D confinement [10]. The electric field from the dielectric glass walls confines the particles horizontally. A temperature gradient in the neutral gas due to the heated lower electrode (55 °C) leads to an upward thermophoretic force that, together with the electric field force, levitates the particle cloud against gravity.

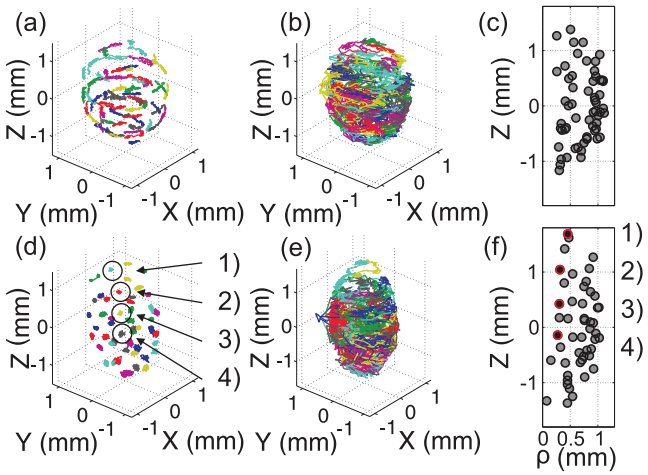

Figure 2. Trajectories over a time span of about 10 s of the $N = 60$ particle cluster for (a) 0 mW laser power, (b) 250 mW laser power and (c) equilibrium particle positions in cylindrical coordinates $\rho = \sqrt{x^2 + y^2}$ and z for case (a). (d)–(f) The same for a $N = 49$ particle cluster which has a structure influenced by the ion focus. A single particle chain is highlighted in (d) and (f), e.g. particles 1–4. See text for details.

In that manner, up to hundred dust grains can be confined in an isotropic potential well where they form ordered 3D structures, the so-called Yukawa balls, see figure 2 and [9, 10]. To follow the kinetics of each individual particle in the cluster, we use the stereoscopic setup described in detail in [23, 27]. The particles are illuminated via two expanded Nd:YAG laser beams at 532 nm with 600 mW power each. Three C-MOS cameras observe the scattered light from the dust from orthogonal directions. Here, they were operated at a frame rate of 100 frames per second. In the experiments here, long runs with up to 30 000 frames per camera were recorded.

Two focused laser beams from diode lasers at 660 nm with maximum output power of 1 W are used to laser-heat the Yukawa balls from two opposing sides. The beams are swept randomly over the cross section of the cluster similar to the procedure of [14, 32], leading to heating primarily in the horizontal direction. In the experiments shown here, the two lasers are adjusted to the same output power with a maximum power of $P_L = 400$ mW at the cloud position. With this setup we are able to heat Yukawa balls with particle numbers $N < 100$ to the liquid regime [14].

We conducted several experiments upon laser heated finite 3D dust clouds by varying the particle number ($5 < N < 100$), the rf power of the discharge and the neutral gas pressure.

It is well known from many dusty plasma experiments that the ion focusing effect becomes important below a certain neutral gas pressure. The ion focus is due to ions flowing through a dust cloud. By the electric field of the dust the ions are focused below the highly charged particles [46]. There, the ions create a local positive space charge, which on the one hand leads to a flow-alignment of particles [47–49, 52–60]. On the other hand, the flow-aligned state can exhibit unstable oscillations, so-called Schweigert instabilities [46]. The trend to form aligned particle chains was reported in various experiments with finite 3D dust clouds confined at low pressure under the influence of an ion focus [12–14, 16, 50, 51, 61].

To study the mode dynamics of Yukawa balls with and without the trend to form aligned particle chains, we choose two representative clusters. Firstly, we have confined and analysed a cluster above the critical neutral gas pressure for the onset of Schweigert oscillations (6.4 Pa and 1.3 W rf power). The Yukawa ball with $N = 60$ particles is spherical in shape and consists of two shells, see figures 2(a)–(c). Secondly, we selected a cluster that was confined at 4.8 Pa and 1.5 W, just below the threshold neutral gas pressure. The cluster with $N = 49$ particles is slightly elongated along the ion streaming direction (aspect ratio about 1.7:1) and the particles tend to align below each other, see figures 2(d)–(f). The four highlighted particles shown in figure 2 build a single vertical chain emphasizing the trend to chain formation.

3. Mode properties

The fluid mode as well as the normal mode technique to analyse the mode properties of finite dust clusters are briefly described. In dimensionless units, the Hamiltonian for the ground state of the N particle ensemble can be written as [7]

$$E = \sum_{i=1}^{N} r_i^2 + \sum_{i<j}^{N} \frac{\exp(-\kappa r_{ij})}{r_{ij}}, \tag{1}$$

where coordinates and energies are dimensionless with the units $r_0 = (Q^2/2\pi\varepsilon_0 m\omega_0^2)^{1/3}$ and $E_0 = (m\omega_0^2 Q^4/32\pi^2\varepsilon_0^2)^{1/3}$. Furthermore ω_0 is the trap frequency, Q and m the dust charge and mass, $r_i = \sqrt{x_i^2 + y_i^2 + z_i^2}$ is the distance of particle i to the trap centre. The indices i and j denote the particles and $\kappa = r_0/\lambda_D$ the screening strength, which is inversely proportional to the Debye length λ_D. The first term in equation (1) describes the isotropic harmonic 3D confinement and the second the pairwise interaction between the charged particles. The interaction is of Yukawa type, since shielding by the ambient plasma should be taken into account.

Although the $N = 49$ cluster confined at low pressure lacks a perfect isotropic shape and even though wake field effects become important for this cluster [50–52], we can test the validity of state of the art theories [4, 8] in the limit of realistic experimental situations.

3.1. Fluid modes analysis

When the number of dust particles becomes sufficiently large, it is convenient to treat the system as a continuum. In addition, when the cluster is not in a solid state, a fluid description might be more adequate.

Kählert and Bonitz [8, 37] treated the Yukawa cluster as a fluid droplet and derived the modes by solving the plasma fluid equations. In their approach, the total potential of the dust cloud with time-dependent density $n_d(\vec{r}, t)$ is expanded into a set of radial and angular eigenfunctions. Multipole moments of the density can be defined in terms of these eigenfunctions as

$$q_{lm}(t) = Q\sqrt{\frac{4\pi}{2l+1}} \int n_d(\vec{r}', t)\hat{i}_l(\kappa r')Y_{lm}^*(\theta, \phi)\mathrm{d}\vec{r}', \tag{2}$$

with l and m being the angular mode numbers, $\hat{i}_l(\kappa r')$ the modified spherical Bessel function, and $Y_{lm}(\theta, \phi)$ the spherical harmonics, respectively. In our analysis, weak screening was

assumed by fixing the screening strength to $\kappa = 0.6$ but other values of κ did not reveal any qualitative differences [23, 24].

In order to derive the experimental fluid modes, the particle positions at each time step are taken to calculate the multipole moments q_{lm}, where the density n_d is treated as a series of δ-functions according to $n_\mathrm{d}(\vec{r}, t) = \sum_i \delta(\vec{r} - \vec{r}_i(t))$. For all fluid modes shown here, we calculated the power spectral density from 30 000 frames. The power spectral density $q_{lm}(\omega)$ of each fluid mode is taken as the Fourier transform of $q_{lm}(t)$ via

$$q_{lm}(\omega) = \frac{2}{TN} \left| \int_0^T q_{lm}(t) \exp(-\mathrm{i}\omega t)\, \mathrm{d}t \right|^2 \tag{3}$$

over a time interval T.

3.2. Normal mode analysis (NMA)

For the sake of a broader picture, the dynamics has also been analysed by normal modes [4, 27, 35, 62, 63]. Thereby, it is assumed that the particles only perform small oscillations around their local equilibrium positions. Thus, using the dynamical matrix, i.e. the second derivative of the total energy given in equation (1),

$$H = \frac{\partial^2 E}{\partial r_{\alpha,i}, \partial r_{\beta,j}}, \tag{4}$$

the $3 \times N$ eigenvalues and eigenvectors are calculated with α and β being the Cartesian coordinates x, y, z and i, j denoting the particle number. The eigenvalues define the frequencies of the different modes of the Yukawa cluster. The resulting 3D eigenvectors $\vec{e}_{i,l}$ describe the oscillation pattern of particle i in each normal mode l.

From the measured time series, the velocities $\vec{v}_i(t)$ of each particle are mapped onto the eigenmode pattern according to

$$f_l(t) = \sum_{i=1}^{N} \vec{v}_i(t)\vec{e}_{i,l}. \tag{5}$$

From this, the NMA spectral power density $S_l(\omega)$, i.e. the energy per frequency interval of each individual crystal mode l, follows from the Fourier transform of equation (5) similar to equation (3) above [27]. Contrary to the fluid mode technique, where the momentary particle positions inside the dust cloud are required, the NMA needs the full trajectories of each individual dust grain. For the NMA performed here, the full 3D trajectories of more than 1600 frames per experiment were used.

While both approaches are well applicable to dust clouds at high pressure, the analysis faces problems at low pressure since both methods are based on the isotropic Yukawa potential. In the latter case, the streaming ions make the potential anisotropic and lead to non-reciprocal inter-particle forces [52]. In principle, the ion focus can be taken into account by introducing an additional positive charge below each dust grain [46, 58, 64, 65] or by using the linear response formalism to calculate an improved interaction potential [50, 52]. However, the anisotropy of the clusters in the present experiment is not very pronounced, which is why we neglect these effects in our analysis. The comparison with the measurements is thus expected to yield useful information on the importance of wake effects in the theoretical description.

4. Results

For the analysis of fluid modes and NMA of Yukawa balls two clusters are considered. The first cluster is of spherical shape. The pressure (6.4 Pa) was high enough to suppress the onset of Schweigert oscillations. The second dust cloud under investigation has aligned particle chains. Here, the cluster was trapped at 4.8 Pa where an influence of the ion streaming motion onto the dust dynamics is expected. Both clusters were laser-heated in the same manner.

4.1. Fluid modes of the spherical dust cluster $N = 60$

We have observed a spherical dust cluster and recorded the particle motion over 30 000 frames. From that, the particle positions have been determined. Then, the spectra of the fluid modes were calculated for all angular mode numbers up to the order $l = m = 5$ according to equations (2) and (3). Here, the q_{00}, q_{10} and q_{11} fluid modes are presented as representatives for the monopole and dipole modes (with q_{00} being breathing mode like [8, 37], q_{10} containing the sloshing mode in vertical direction and q_{11} containing the sloshing mode in horizontal direction). As examples for fluid modes with a more complex structure, the spectra of the q_{2m}, $m = 0, 1, 2$ modes are depicted, corresponding to quadrupole modes.

Figure 3(a) shows the spectra of the fluid modes q_{00}, q_{10} and q_{11} and figure 3(b) the spectra of the fluid modes q_{20}, q_{21} and q_{22} for the unheated $N = 60$ cluster. Figures 3(c) and (d) show the same modes for the same cluster in the liquid regime at a laser heating power of $P_{\mathrm{L}} = 250$ mW. In the absence of any external laser heating, figures 3(a) and (b), no fluid modes are detectable.

For the spectra of the heated cluster shown in figures 3(c) and (d), mainly two fluid modes are excited. This can be seen from the elevated signal of the q_{11} fluid mode at 2.5 Hz and the q_{22} fluid mode at 3.0 Hz. The value of the peak positions for all fluid modes shown here and in the following were determined by fitting a Gaussian distribution to the peak. The peak width was typically found from the fit as $\sigma = 1.4$ Hz. The reason for the excitation of the horizontal q_{11} and q_{22} modes can be understood by the fact that the beams are pointing in the horizontal direction to the dust cloud. Therefore, the lasers transfer momentum to the cluster particles mainly in this direction.

Interestingly, the ratio of the two mode frequencies $\omega_{22}/\omega_{11} = f_{22}/f_{11} = 3.0/2.5\,\mathrm{Hz} = 1.2$, is in good agreement with the fluid theory which predicts two limiting cases: (a) for $\kappa = 0$ one gets $\omega_{ll} = \sqrt{3l/2l+1}\omega_0$, $\omega_{22}/\omega_{11} = \sqrt{3 \cdot 2/(2 \cdot 2+1)} = 1.095$ and for (b) $\kappa \to \infty$ one finds $\omega_{ll} = \sqrt{l}\omega_0$, $\omega_{22}/\omega_{11} = \sqrt{2} \approx 1.41$ [8]. In particular, equating the theoretical ratio to 1.2 we obtain $\kappa = 0.57 \approx 0.6$, which is in good agreement with earlier findings (due to the weak dependence of the frequency on the screening parameter (see figure 2 in [8]), the error is relatively large).

A possible cause not to find any peak in the q_{00} spectra (which describes a monopole breathing oscillation) is the presence of neutral drag. As pointed out by Kählert and Bonitz low damping rates are necessary to detect fluid modes [37]. In our experiment, the neutral gas pressure was held constant at 6.4 Pa. From this, the Epstein friction coefficient can be calculated as $\nu = 8\,\mathrm{s}^{-1}$ [66]. When we now assume that the peak of the q_{11} mode is a sloshing oscillation at the trap frequency $f_{11} = 2.5\,\mathrm{Hz} \approx \omega_0/(2\pi)$ the normalized friction is $\nu/\omega_0 \approx 0.5$. Even though the gas pressure is relatively low compared to most other Yukawa ball experiments [22, 23, 27], only a few broad peaks can be seen in the interesting frequency domain.

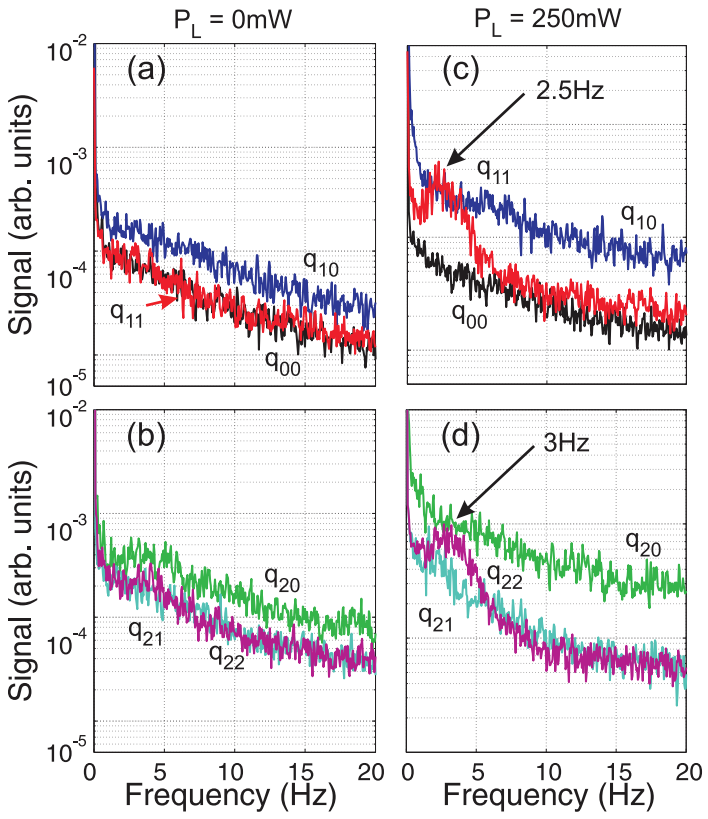

Figure 3. Spectra of fluid mode analysis of a spherical $N = 60$ particle cluster. Spectra of fluid modes q_{00}, q_{10} and q_{11} in (a) and q_{20} to q_{22} in (b) for the unheated cluster. Spectra of fluid modes q_{00}, q_{10} and q_{11} in (c) and q_{20} to q_{22} in (d) for the cluster in the liquid regime ($P_L = 250$ mW). The unheated cluster does not show any characteristics at all. The laser heated cluster has a transverse sloshing mode q_{11} at 2.5 Hz and a transverse quadrupole mode q_{22} at 3.0 Hz.

4.2. Fluid modes of the wake-affected dust cluster $N = 49$

It is tempting to reduce the neutral gas pressure in order to decrease friction of the particles. This should lead to richer fluid mode spectra [37]. As discussed in section 2, lowering the neutral gas pressure leads to an increasing influence of the ion focus on the particles [36, 49]. Thus, we can study the influence of damping and the influence of anisotropic particle–particle interactions to the fluid modes at once. The spectra of the same fluid modes as above are shown in figure 4 for a cluster with $N = 49$ particles to compare directly with the results of the isotropic cluster.

In the absence of any external laser heating, figures 4(a) and (b), indeed a few collective excitations appear in the elongated cluster. No peak occurs in spectra of the q_{00} and q_{10} fluid mode. An elevated signal can be found in the q_{11} mode at about 3.5 Hz. The q_{22} fluid mode, which represents a transverse quadrupole oscillation, has also a broad peak at the frequency domain of 4 Hz. Moreover, a sharp peak occurs in all quadrupole spectra and in nearly all spectra of the higher order modes at 7.8 Hz for this cluster indicating that this peak is not a pure fluid eigenmode.

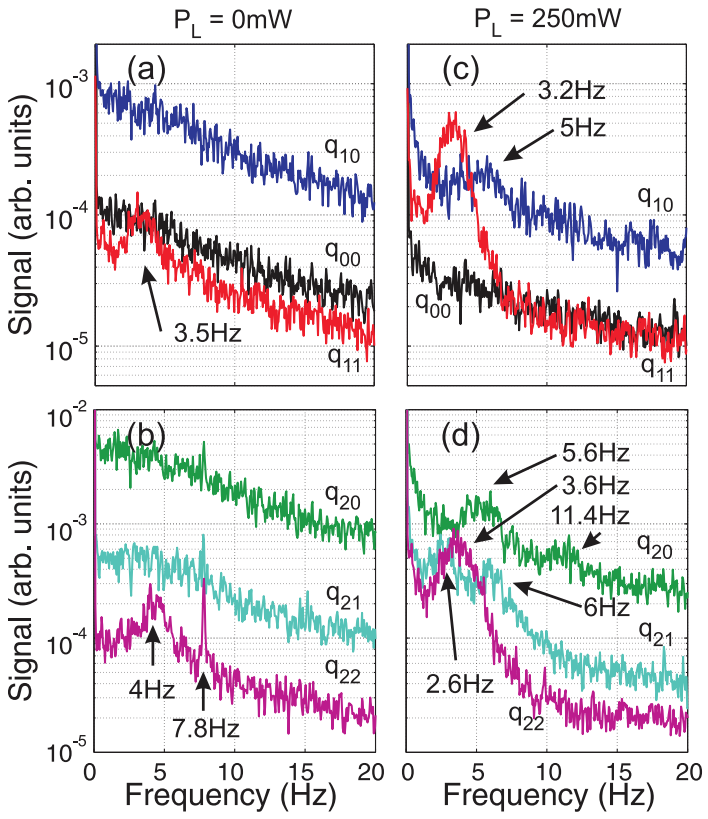

Figure 4. Spectra of fluid mode analysis of an elongated $N = 49$ particle cluster as in figure 3. Laser heating destroys the ion focus related unstable oscillation at 7.8 Hz and mainly excites a sloshing movement at 3.2 Hz.

Even though the friction is rather low no q_{00} mode is detectable (for 4.8 Pa and assuming the trap frequency to be $\omega_0/(2\pi) \approx 3.5$ Hz one finds $\nu/\omega_0 \approx 0.27$). The reason is in the elongation of the cluster along the z-axis and the particle-interaction, which is influenced by the ion focus. Such a cluster does not possess a uniform monopole mode.

High mode numbers generally correspond to more localized oscillations in the cluster. The observed sharp peak at 7.8 Hz in the spectra of the higher-order fluid modes for the $N = 49$ cluster thus belongs to an oscillation that does not involve large-scale motion. Moreover, the fact that quadrupole oscillations transverse to the ion flow q_{22} are favoured over the longitudinal quadrupole oscillations seem to confirm that restoring forces are mainly in the direction perpendicular to the ion streaming direction even without laser excitation [48, 49, 60].

The origin of the transverse restoring forces can be attributed to the ion focus [46, 48, 49, 60]. The alignment can result in unstable oscillations—the Schweigert instability—since there are repulsive forces between the dust particles and attractive forces between ion cloud and the dust particles [47, 48, 52–59].

Additional evidence for the Schweigert instability in our experiment is given by the fact that the dust system is 'heated' by the instability [14, 31, 36, 46, 58, 64, 67–69]. For the dust cluster under investigation, the temperature (mean kinetic energy) of the cluster particles is found at $T_{\mathrm{kin}} = m\left\langle v^2\right\rangle/3k_{\mathrm{B}} \approx 7370$ K, i.e. far above room temperature even in the unheated case [14, 67]. For comparison, the cluster in section 4.1 has $T = 2930$ K.

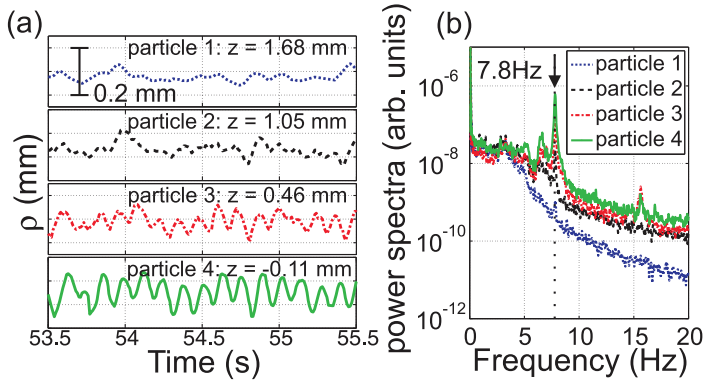

Figure 5. (a) Transverse movement of selected particles in the cluster over a time span of 2 s. All particles belong to one particle chain where the particles are numbered from top to bottom. The correlated oscillatory movement of particles 2–4 is clearly visible. (b) The corresponding power spectra from the full trajectories (300 s), showing a peak in the spectra at 7.8 Hz.

To underline the above argument, the motion of individual particles was analysed. Therefore, the four representative particles of the particle chain were chosen (marked in figure 2).

In figure 5(a) the transverse (to the ion stream) movement $\rho(t)$ of the four particles within the cluster is shown over a time span of 2 s. The corresponding power spectra from the full trajectories (300 s) are depicted in figure 5(b).

For the uppermost particle 1, the trajectory does not show any particular oscillations, consequently the power spectrum is nearly flat. In contrast, the lower particles 2–4 respond to the ion wakefield from particles placed above it. This can be seen from the trajectories correlated oscillatory motion and the corresponding peak in the spectra of the particles, respectively. Clearly, the frequency of the peak in the spectrum of the individual particle motion $\rho(t)$ coincides with that of the q_{2m} fluid modes. Furthermore, the amplitude of the oscillatory motion increases with particle positions further down the ion stream. This supports that these oscillations are due to the Schweigert instability. A second peak in the spectrum for particles 3 and 4 at the first harmonic ($\approx$16 Hz) hints at the nonlinear character of these oscillations.

The ion wakes induce local small-scale perturbations of the cloud potential, leading to signals in the fluid spectra for higher mode numbers, see figure 4. Even when the fluid mode technique starts from the assumption of an isotropic Yukawa model, equation (1), it allows for identification of such instabilities.

To display the influence of heating, the fluid mode spectra for the laser heated $N = 49$ cluster are shown in figures 4(c) and (d). Heating was applied in the same manner as for the spherical cluster. Here, the peak at roughly 3.2 Hz is even more pronounced in the q_{11} mode. A slightly higher signal is also found in the spectra of the q_{10} mode at 5 Hz.

Contrary to the unheated case, no sharp peaks occur at 7.8 Hz for higher angular mode numbers $l = 2$. Instead, several other modes are excited at 5.6 and 11.4 Hz in the q_{20} mode, at 2.6 and 6 Hz in the q_{21} mode and at roughly 3.6 Hz in the q_{22} fluid mode.

The ratio of the two mode frequencies $\omega_{22}/\omega_{11} = 4/3.5\,\text{Hz} = 1.14$ for the unheated, and 3.6/3.2 Hz = 1.13 for the heated case, respectively, agree well with the ratio for the spherical cluster and literature [8]. However, one must take into account that the assumptions of the theory, i.e., isotropic confinement and interaction, are not fully fulfilled here.

According to the fluid theory of [8], the frequency for excitations in the q_{lm} fluid modes for the same l but different m should be independent of mode number m, since the underlying theory assumes isotropic confinement and isotropic particle–particle interaction. The fact that the frequencies of the q_{1m} and q_{2m} fluid modes change as m changes could either indicate that the confinement in the experiment is not perfectly isotropic or that the symmetry in the particle–particle interaction is broken due to the presence of an ion focus.

4.3. Evolution of fluid modes during laser heating

To analyse the fluid behaviour of finite dust clouds more closely, the evolution of the q_{11} mode and the q_{22} mode with temperature is investigated. Here, we restrict to the $N = 49$ cluster, since the fluid modes are more pronounced than for the spherical cluster, but the general results are qualitatively the same. The mode evolution is shown in figure 6 as a function of laser heating power. The power of the two beams was varied between 0 and 400 mW in steps of 50 mW thus covering a wide range of fluidity.

For comparison, the kinetic temperature of the cluster particles as function of the applied laser power is shown in figure 6(c) together with the corresponding Coulomb coupling parameter. The Wigner–Seitz radius for the $N = 49$ cluster was estimated as $b_{\text{WS}} = (3/4\pi n)^{1/3} = 340\,\mu\text{m}$ from the overall density. For the dust charge, the value of [14] $Q = 6900e$ was used. The solid curve represents a parabolic fit of the temperature versus laser heating power. This parabolic dependence corresponds to a laser particle interaction via radiation pressure [38, 70]. It was shown previously [14] that the velocity distribution is not purely Maxwellian for the dust particles, but sufficient to assign a temperature to the 3D dust clusters.

In each spectrum of the q_{11} fluid mode shown in figure 6(a), a peak is found at a frequency range of (3.3±0.2) Hz. The position of the peak maximum does not change significantly with laser heating. This transverse sloshing mode was already discussed in the previous section. The peak height slightly increases as the laser power increases, and the peak gets broader. This is exactly what is expected for the fluid modes [37].

Figure 6(b) shows the evolution of the q_{22} fluid mode. Here, a peak is found for all modes at a frequency interval of about (3.7±0.2) Hz. As in figure 6(a), the peak height increases and broadens continuously. Similar behaviour was found for all fluid modes. The oscillation associated with the Schweigert instability at 7.8 Hz is seen for the unheated cluster at 0 mW. At higher heating this peak is destroyed, probably due to the frequent particle exchanges in the liquid regime.

4.4. NMA of finite dust clusters

One goal of this paper is to compare the fluid and crystal modes of finite dust clouds. Contrary to the fluid mode description, where the Yukawa ball is treated like a fluid droplet, the NMA describes the harmonic movement of individual dust grains in terms of crystal modes [4, 71]. To compare the crystal modes with the fluid mode results, a NMA is performed from the trajectories of the spherical and the aligned cluster for the unheated crystalline case ($P_{\text{L}} = 0\,\text{mW}$) and

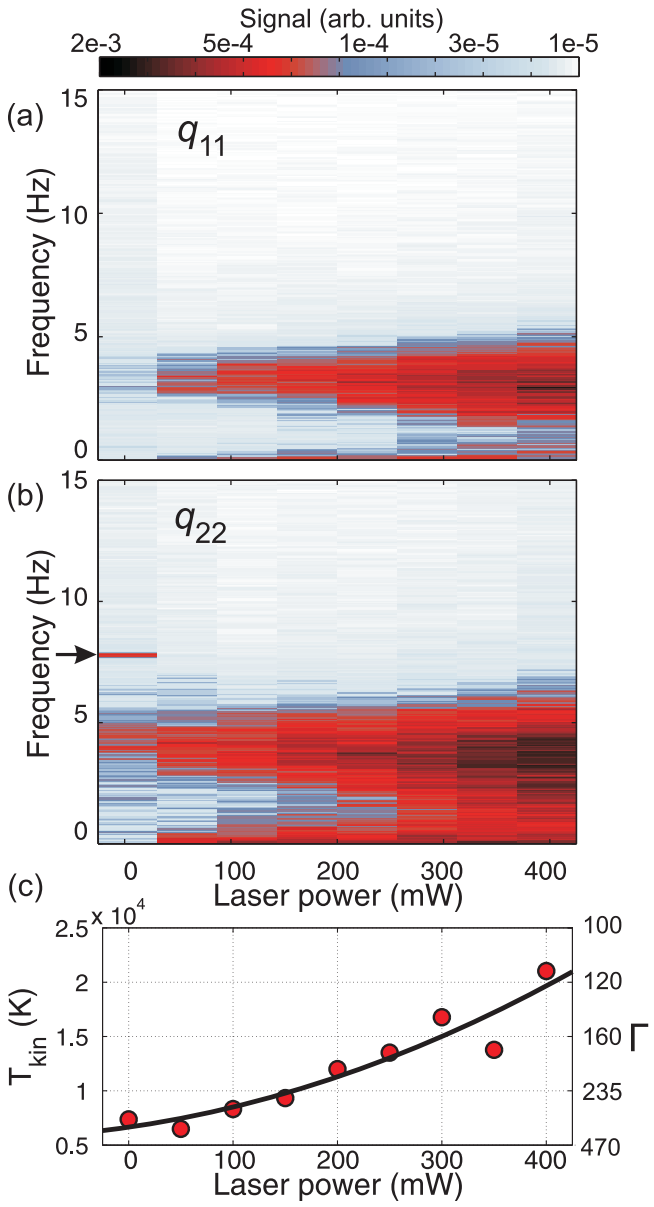

Figure 6. Evolution of the q_{11} fluid mode (a) and the q_{22} fluid mode (b) during laser heating. In (c) the kinetic temperature of the cluster particles and the Coulomb coupling strength for the applied laser power are shown. The solid curve corresponds to a parabolic fit.

the heated, liquid-like clusters ($P_L = 250\,\mathrm{mW}$). For both cases, the 3D positions of the cluster particles with respect to the centre of mass were assumed to be equilibrium positions and again weak screening $\kappa = 0.6$ was assumed to calculate the dynamical matrix H of equation (4).

The reason for choosing the NMA instead of the recently established instantaneous normal mode (INM) technique is that the NMA allows to investigate the mode resolved spectral properties, whereas the INM only enables to reveal information about the total distribution of the eigenfrequencies [32, 72].

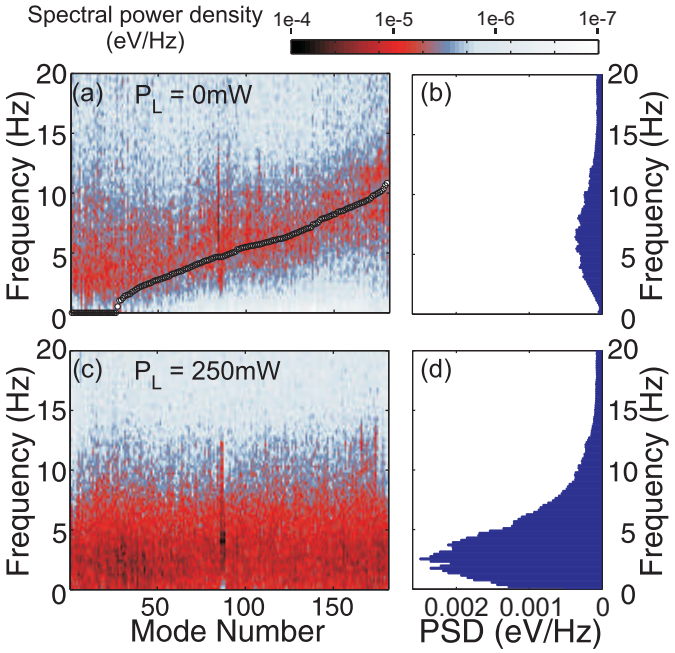

Figure 7. Normal mode spectra for the spherical $N = 60$ particle cluster ($p = 6.4$ Pa); (a) power spectral density per mode and (b) corresponding PSD for the unheated cluster, (c) power spectral density per mode and (d) corresponding PSD for a cluster in the liquid regime ($P_L = 250$ mW). In the mode resolved spectra, darker colours correspond to a higher energy per frequency interval. The circles correspond to calculated mode frequencies. Without external heating, the energy per mode is concentrated in an narrow frequency band.

Figure 7 shows the mode resolved NMA spectral power density for the unheated cluster and the heated cluster together with the total power density $S(\omega)$ (PSD), which follows from the summing up $S_l(\omega)$ over each individual mode $S(\omega) = \sum_l S_l(\omega)$.

For the crystalline cluster, figure 7(a), regions with higher power density can be found for each mode. These regions shift slightly to higher frequencies as the mode number increases. This is the expected trend and has been previously demonstrated for 2D and 3D clusters [27, 36]. The spectral width is much less than that of [27] due to the much lower pressure used in the present experiment. The corresponding PSD, figure 7(b), that is obtained from the integration over all modes, shows evenly distributed energy at each frequency in this representation. However, the interpretation of individual normal modes is not as straightforward as in the fluid mode description. For the heated cluster, see figure 7(c), the energy in the modes is not located in a narrow frequency band as for the solid cluster. Higher energy can be found in a much broader region up to 15 Hz for all modes. In the PSD, figure 7(d), most of the energy in the system is seen to be located in a broad frequency range with its maximum at about 2.6 Hz. Compared to the PSD for the solid cluster, figure 7(b), laser heating increases the values of the PSD about one order of magnitude since kinetic energy is deposited to the cluster particles. Frequent particle exchanges occurring in this liquid regime prevent the establishment of normal mode oscillations. Thus, the spectrum is much broader as for the cluster in the solid phase, so as the NMA is mainly suited for crystalline states.

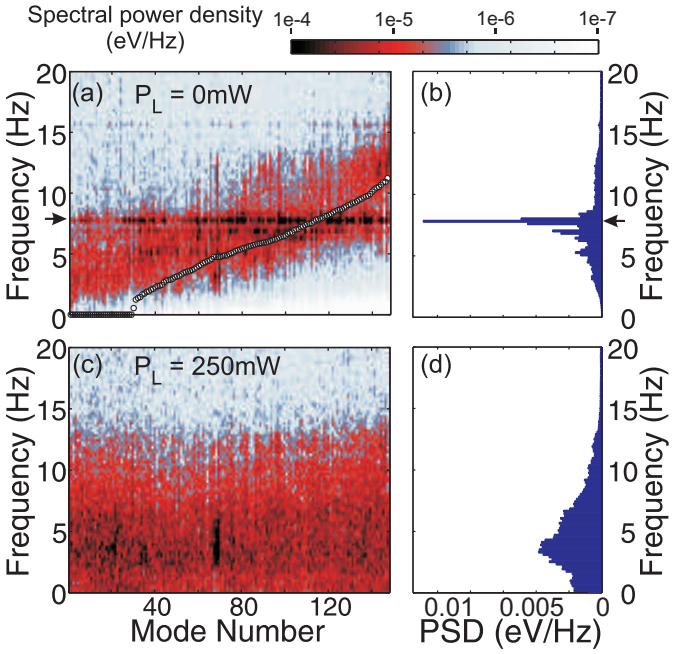

Figure 8. Normal mode spectra for the wake-affected $N = 49$ particle cluster ($p = 4.8$ Pa) as in figure 7. In the unheated case, an unstable oscillation occurs at 7.8 Hz within all modes (marked by the arrows).

The $N = 49$ cluster with aligned particle chains was investigated by means of NMA in the same manner as described above. For the solid cluster, figure 8(a), the features of the mode resolved NMA spectra of a solid weakly damped Yukawa cluster are recovered, too. Moreover, in this unheated case, a significant amount of energy is stored in a narrow frequency band around 7.8 Hz in most of all modes. Consequently, this feature is no eigenmode of the system [36]. The peak at 7.8 Hz becomes more distinct in the corresponding PSD, see figure 8(b). The contribution at 7.8 Hz is by far the most dominant input in the PSD (note that energy density in this narrow frequency band is about two magnitudes larger than for the unheated spherical cluster, figure 7). Thus, the Schweigert instability at 7.8 Hz can be identified within both, the crystal and the fluid mode approach.

The mode resolved NMA spectra of the heated chain-like cluster, see figure 8(c), looks very similar to that of the spherical cluster with laser heating. In the PSD, figure 8(d), the maximum of the energy is now found at 3.3 Hz due to the different discharge parameters.

It is a remarkable result that even when both approaches assume isotropy and use different data as an input (fluid modes require the 3D density, i.e. the particle positions, and NMA uses the particles velocities), the dominant spectral properties of the system are well recovered:

In the fluid regime, the peak of the q_{11} fluid mode coincides with the maximum of the PSD for both clusters. Moreover, in the unheated case of the elongated cluster, the sharp peak at 7.8 Hz due to the ion focus is covered by the NMA and the fluid mode approach as well. A difference in both methods lies however in the allocation of the total energy of the system onto the individual crystal or fluid modes.

5. Summary

A comparison between two different approaches, the NMA and the fluid mode technique, describing the mode structure of finite 3D Yukawa type systems in solid and liquid phases was made. For that purpose, a cluster consisting of $N = 60$ particles representing a spherical Yukawa ball and a cluster formed from $N = 49$ particles, which was elongated along the ion streaming direction, were investigated. Both clusters, which were solid in the unheated case, were gradually heated by means of two opposing laser beams to a liquid state.

The fluid mode technique was applied to the experimental data. Here, the dust cluster is treated as a continuous fluid, similar to a fluid droplet. Diverse fluid modes could be identified in the motion of the finite dust clouds. Furthermore, for the crystalline but elgonated cluster, the Schweigert instability at 7.8 Hz was seen as a sharp peak in high order modes, that corresponds to more local cloud oscillations.

Transverse laser heating mainly excites fluid modes that correspond to a transverse particle movement. The evolution of fluid modes was followed during laser heating. The mode frequencies were found to be nearly independent of heating power, but the peaks themselves were getting broader, in agreement with theoretical calculations.

A NMA was performed to compare the fluid modes with crystal eigenmodes. A clear mode spectrum has been derived for the unheated, crystal-like 3D clusters. Again, it has been revealed that the ion focus leads to an unstable oscillation of the cluster particles due to the Schweigert instability for the cluster which leads to particle alignment. With laser heating, i.e. when the clusters are in a liquid-like regime, the NMA spectra becomes less structured due to frequent particle exchanges.

Both methods yield comparable results concerning the spectral features of the system, even for the low particle numbers of the investigated cluster and under the influence of the ion focus. Also, both techniques hint at the non-isotropy of the confinement and particle interaction.

The results are a helpful input and feedback for theory and simulations. Future extensions of the theory, for instance for systems in a flowing environment, are desirable, as they are important for a quantitative comparison. This will allow to widen up the fluid mode description to a broader area of physical systems, even beyond dusty plasmas.

Acknowledgments

This work was supported by the Helmholtz Gemeinschaft via HEPP and by the Deutsche Forschungsgemeinschaft via SFB-TR24 projects A3, A7 and A9.

References

[1] Morfill G E, Ivlev A V and Thomas H M 2012 *Phys. Plasmas* **19** 055402
[2] Bonitz M, Horing N and Ludwig P (ed) 2010 *Introduction to Complex Plasmas* (*Springer Series on Atomic, Optical and Plasma Physics*) (Berlin: Springer)
[3] Shukla P K and Mamun A A 2002 *Introduction to Dusty Plasma Physics* (Bristol: Institute of Physics Publishing)
[4] Schweigert V A and Peeters F M 1995 *Phys. Rev.* B **51** 7700
[5] Schiffer J P 2002 *Phys. Rev. Lett.* **88** 205003
[6] Böning J, Filinov A, Ludwig P, Baumgartner H, Bonitz M and Lozovik Y E 2008 *Phys. Rev. Lett.* **100** 113401

[7] Bedanov V M and Peeters F M 1994 *Phys. Rev.* B **49** 2667
[8] Kählert H and Bonitz M 2010 *Phys. Rev.* E **82** 036407
[9] Arp O, Block D, Piel A and Melzer A 2004 *Phys. Rev. Lett.* **93** 165004
[10] Arp O, Block D, Klindworth M and Piel A 2005 *Phys. Plasmas* **12** 122102
[11] Flanagan T M and Goree J 2009 *Phys. Rev.* E **80** 046402
[12] Kroll M, Schablinski J, Block D and Piel A 2010 *Phys. Plasmas* **17** 013702
[13] Killer C, Schella A, Miksch T and Melzer A 2011 *Phys. Rev.* B **84** 054104
[14] Schella A, Miksch T, Melzer A, Schablinski J, Block D, Piel A, Thomsen H, Ludwig P and Bonitz M 2011 *Phys. Rev.* E **84** 056402
[15] Kong J, Hyde T W, Matthews L, Qiao K, Zhang Z and Douglass A 2011 *Phys. Rev.* E **84** 016411
[16] Wörner L, Räth C, Nosenko V, Zhdanov S K, Thomas H M, Morfill G E, Schablinski J and Block D 2012 *Europhys. Lett.* **100** 35001
[17] Hyde T W, Kong J and Matthews L S 2013 *Phys. Rev.* E **87** 053106
[18] Henning C, Baumgartner H, Piel A, Ludwig P, Golubnichiy V, Bonitz M and Block D 2006 *Phys. Rev.* E **74** 056403
[19] Henning C, Ludwig P, Filinov A, Piel A and Bonitz M 2007 *Phys. Rev.* E **76** 036404
[20] Baumgartner H, Kählert H, Golobnychiy V, Henning C, Käding S, Melzer A and Bonitz M 2007 *Contrib. Plasma Phys.* **47** 281
[21] Baumgartner H, Golobnychiy V, Asmus D, Ludwig P and Bonitz M 2008 *New J. Phys.* **10** 093019
[22] Block D, Käding S, Melzer A, Piel A, Baumgartner H and Bonitz M 2008 *Phys. Plasmas* **15** 040701
[23] Käding S, Block D, Melzer A, Piel A, Kählert H, Ludwig P and Bonitz M 2008 *Phys. Plasmas* **15** 073710
[24] Kählert H, Ludwig P, Baumgartner H, Bonitz M, Piel A, Block D and Melzer A 2008 *Phys. Rev.* E **78** 036408
[25] Melzer A, Käding S, Block D and Piel A 2008 *J. Phys.: Condens. Matter* **20** 404204
[26] Kählert H and Bonitz M 2010 *Phys. Rev. Lett.* **104** 015001
[27] Ivanov Y and Melzer A 2009 *Phys. Rev.* E **79** 036402
[28] Apolinario S, Partoens B and Peters F 2007 *New J. Phys.* **9** 283
[29] Antonova T, Annaratone B M, Goldbeck D D, Yaroshenko V, Thomas H M and Morfill G E 2006 *Phys. Rev. Lett.* **96** 115001
[30] Antonova T, Annaratone B M, Thomas H M and Morfill G E 2008 *New J. Phys.* **10** 043028
[31] Aschinger A and Winter J 2012 *New J. Phys.* **14** 093036
[32] Schella A, Mulsow M, Melzer A, Schablinski J and Block D 2013 *Phys. Rev.* E **87** 063102
[33] Lisin E A, Timirkhanov R A, Vaulina O S, Petrov O F and Fortov V E 2013 *New J. Phys.* **15** 053004
[34] Kalman G J, Hartmann P, Donkó Z, Golden K I and Kyrkos S 2013 *Phys. Rev.* E **87** 043103
[35] Melzer A, Klindworth M and Piel A 2001 *Phys. Rev. Lett.* **87** 115002
[36] Ivanov Y and Melzer A 2005 *Phys. Plasmas* **12** 072110
[37] Kählert H and Bonitz M 2011 *Phys. Rev.* E **83** 056401
[38] Wolter M and Melzer A 2005 *Phys. Rev.* E **71** 036414
[39] Nosenko V, Goree J and Piel A 2006 *Phys. Plasmas* **13** 032106
[40] Nosenko V, Zhdanov S K, Ivlev A V, Knapek C A and Morfill G E 2009 *Phys. Rev. Lett.* **103** 015001
[41] Feng Y, Goree J and Liu B 2010 *Phys. Rev. Lett.* **104** 165003
[42] Schablinski J, Block D, Piel A, Melzer A, Thomsen H, Kählert H and Bonitz M 2012 *Phys. Plasmas* **19** 013705
[43] Thomsen H, Kählert H, Bonitz M, Schablinski J, Block D, Piel A and Melzer A 2012 *Phys. Plasmas* **19** 023701
[44] Feng Y, Goree J and Liu B 2012 *Phys. Rev.* E **85** 066402
[45] Nosenko V, Ivlev A V and Morfill G E 2013 *Phys. Rev.* E **87** 043115
[46] Schweigert V A, Schweigert I V, Melzer A, Homann A and Piel A 1996 *Phys. Rev.* E **54** 4155
[47] Melzer A, Schweigert V and Piel A 1999 *Phys. Rev. Lett.* **83** 3194
[48] Piel A 2011 *Phys. Plasmas* **18** 073704

[49] Hutchinson I H 2012 *Phys. Rev.* E **85** 066409
[50] Ludwig P, Miloch W J, Kählert H and Bonitz M 2012 *New J. Phys.* **14** 053016
[51] Block D, Carstensen J, Ludwig P, Miloch W J, Greiner F, Piel A, Bonitz M and Melzer A 2012 *Contrib. Plasma Phys.* **52** 804–12
[52] Lampe M, Joyce G and Ganguli G 2005 *IEEE Trans. Plasma Sci.* **33** 57–69
[53] Hutchinson I H 2011 *Phys. Plasmas* **18** 032111
[54] Takahashi K, Oishi T, Shimomai K I, Hayashi Y and Nishino S 1998 *Phys. Rev.* E **58** 7805
[55] Lampe M, Joyce G and Ganguli G 2000 *Phys. Plasmas* **7** 3851–61
[56] Steinberg V, Sütterlin R, Ivlev A V and Morfill G 2001 *Phys. Rev. Lett.* **86** 4540–3
[57] Samarian A A, Vladimirov S V and James B 2005 *JETP Lett.* **82** 858
[58] Couëdel L, Nosenko V, Ivlev A V, Zhdanov S K, Thomas H M and Morfill G E 2010 *Phys. Rev. Lett.* **104** 195001
[59] Hutchinson I H 2011 *Phys. Rev. Lett.* **107** 095001
[60] Arp O, Goree J and Piel A 2012 *Phys. Rev.* E **85** 046409
[61] Ludwig P, Kählert H and Bonitz M 2012 *Plasma Phys. Control. Fusion* **54** 045011
[62] Melzer A 2006 *Phys. Rev.* E **73** 056404
[63] Henning C, Kählert H, Ludwig P, Melzer A and Bonitz M 2009 *J. Phys. A: Math. Theor.* **42** 214023
[64] Zhdanov S K, Ivlev A V and Morfill G E 2009 *Phys. Plasmas* **16** 083706
[65] Carstensen J, Greiner F, Block D, Schablinski J, Miloch W J and Piel A 2012 *Phys. Plasmas* **19** 033702
[66] Epstein P S 1924 *Phys. Rev.* **23** 710–33
[67] Melzer A, Homann A and Piel A 1996 *Phys. Rev.* E **53** 2757
[68] Schweigert V A, Schweigert I V, Melzer A, Homann A and Piel A 1998 *Phys. Rev. Lett.* **80** 5345
[69] Ivlev A, Konopka U, Morfill G and Joyce G 2003 *Phys. Rev.* E **68** 026405
[70] Liu B, Goree J, Nosenko V and Boufendi L 2003 *Phys. Plasmas* **10** 9
[71] Dubin D H E and Schiffer J P 1996 *Phys. Rev.* E **53** 5249–67
[72] Melzer A, Schella A, Schablinski J, Block D and Piel A 2012 *Phys. Rev. Lett.* **108** 225001